High Pressure Inside Nanometer-Sized Particles Influences the Rate and Products of Chemical Reactions

Matthieu Riva, Jianfeng Sun, V. Faye Mcneill, Charline Ragon, Sebastien Perrier, Yinon Rudich, Sergey Nizkorodov, Jianmin Chen, Frédéric Caupin, Thorsten Hoffmann, et al.

High pressure inside nanometre-sized particles influences the rate and products of chemical reactions

Matthieu Riva[†,*], Jianfeng Sun[†,§], V. Faye McNeill[‖], Charline Ragon[†], Sebastien Perrier[†], Yinon Rudich[⊥], Sergey A. Nizkorodov[#], Jianmin Chen[§], Frederic Caupin[▽], Thorsten Hoffmann[○,*], Christian George[†,*]

[†] Univ. Lyon, Université Claude Bernard Lyon 1, CNRS, IRCELYON, F-69626, Villeurbanne, France.

[§] Shanghai Key Laboratory of Atmospheric Particle Pollution and Prevention (LAP3), Department of Environmental Science & Engineering, Fudan University, Shanghai 200433, China.

[‖] Department of Chemical Engineering and Department of Earth and Environmental Sciences, Columbia University, New York, NY 10025 USA

[⊥] Department of Earth and Planetary Sciences, Weizmann Institute, Rehovot 76100, Israel.

[#] Department of Chemistry, University of California, Irvine, CA 92694, USA.

[▽]Université de Lyon, Université Claude Bernard Lyon 1, CNRS, Institut Lumière Matière, F-69622, Villeurbanne, France.

[○] Department of Chemistry, Johannes Gutenberg-Universität, Mainz, Germany.

Keywords: SOA, mass spectrometry, heterogeneous chemistry, pressure, new particle formation

Abstract

The composition of organic aerosol has a pivotal influence on aerosol properties such as toxicity, and cloud droplets formation capability, which could affect both climate and air quality. However, a comprehensive and fundamental understanding of the chemical and physical processes that occur in nanometre-sized atmospheric particles remains a challenge that severely limits the quantification and predictive capabilities of aerosol formation pathways. Here, we investigated the effects of a fundamental and hitherto unconsidered physical property of nanoparticles – the Laplace pressure. By studying the reaction of glyoxal with ammonium sulphate, both ubiquitous and important atmospheric constituents, we show that high pressure can significantly affect the chemical processes that occur in atmospheric ultrafine particles (i.e., particles < 100 nm). Using high-resolution mass spectrometry and UV/Vis spectroscopy, we demonstrated that the formation of reaction products is strongly (i.e., up to a factor of 2) slowed down under high pressures typical of atmospheric nanoparticles. A size-dependent relative rate constant is determined and numerical simulations illustrate the reduction in the production of the main glyoxal reaction products. These results established that the high pressure inside nanometre-sized aerosols must be considered as a key property that significantly impacts chemical processes that govern atmospheric aerosol growth and evolution.

Short Synopsis

High pressure reached inside atmospheric nanometre-sized particles affects their chemistry and therefore their formation and growth.

Introduction

Aerosol particles are a ubiquitous component of the atmosphere, comprising small liquid and solid particles suspended in the air, with diameters that vary from a few nanometres (nm) to several tens of micrometres (μm).[1] Fine atmospheric aerosols ($PM_{2.5}$, particles with aerodynamic diameter ≤ 2.5 μm) produce a significant cooling effect in the atmosphere[1–3] through two mechanisms: by directly reflecting solar radiation back into space, and by acting as nuclei for the formation of cloud droplets, thereby regulating cloud reflectivity and lifetime.[2,3] $PM_{2.5}$ also has a negative impact on air quality and human health, representing the fifth ranking human health risk factor globally.[4] Fine atmospheric aerosols can either be emitted directly into the air as primary aerosol, or formed in the atmosphere by gas-to-particle conversion and classified as secondary aerosol.[1,5] The chemical composition of primary and secondary aerosols is mainly dominated by organic and inorganic species (and water at high relative humidity).While the inorganic species are limited to a few compounds (e.g., sulphates and nitrates are the largest contributors to submicron aerosol mass globally), there are thousands of organic compounds in aerosols.[6] The organic vapours able to grow aerosols by condensation, thus forming "secondary organic aerosol" (SOA), are primarily formed through gas-phase oxidation of volatile organic compounds (VOC) emitted from biogenic and anthropogenic sources.[1,5] However, the precise components and physicochemical processes involved remain poorly understood. Improving our fundamental knowledge of the chemical and physical processes that govern atmospheric aerosol growth and evolution is crucial to better quantify aerosol growth and properties and hence the effect of aerosols on climate change and impact on air quality.

While research is mainly focused on elucidating the processes that control the formation and evolution of SOA, one of the most fundamental properties – the pressure inside atmospheric particles – is currently neglected in aerosol formation and growth models. The Laplace pressure is of central importance for the thermodynamic description of liquids with strongly curved interfaces (i.e., nanoparticles and nanoscale droplets). It represents the pressure difference of a droplet between the inside and outside. This effect is produced due to surface tension at the interface between a liquid and the gas interface of a curved surface.[7] The Laplace pressure is proportional to the surface tension and

65 the inverse of the droplet size.[7] The pressure is a fundamental physical quantity that affects the values
66 of various thermodynamic and kinetic constants of numerous chemical reactions.[8] The crucial
67 parameters to describe the influence of pressure on chemical reactions can be further broken down,
68 namely the reaction volume (ΔV) and the volume of activation ($\Delta^{\ddagger}V$). The volume of activation $\Delta^{\ddagger}V$ is
69 the volume change of the reaction system from the reactants to transition state, and the reaction
70 volume ΔV is the corresponding volume change from the reactants to the products. The former has
71 been studied in particular by Evans and Polanyi in their development of the transition state theory.[9] As
72 a result, the Laplace pressure is expected to have strong effects on the equilibrium state of any
73 chemical system and may either accelerate or slow a given reaction. In general, processes that lead to a
74 net increase in the molar volume from reactants to products (i.e., $\Delta V>0$) are thermodynamically
75 suppressed at high pressure, and processes with a positive volume of activation from reactants to
76 transition state are kinetically suppressed at high pressures.[10]
77 To investigate the influence of the internal pressure on atmospherically relevant systems, we
78 have considered a well-studied reaction of glyoxal and ammonium sulphate. Glyoxal is among the
79 most abundant oxygenated VOC produced in the atmosphere from the oxidation of biogenic and
80 anthropogenic organic precursors.[11] While it was previously considered as too volatile to contribute to
81 SOA formation, recent studies have shown that glyoxal and other small dicarbonyl species can
82 significantly contribute to SOA growth through multiphase chemistry.[12–18] Since these species are
83 largely produced in the gas phase, condensed phase sinks help explaining an important part of the
84 missing SOA mass predicted by simulations.[17,23] In the presence of ammonium sulphate these
85 multiphase processes produce light-absorbing complex organic compounds, that contain an imidazole
86 function.[12,19,20,24] The vast majority of the kinetic studies characterizing atmospheric chemical
87 reactions are conducted in bulk solution,[22]and/or in large aerosols,[18] hence earlier studies on glyoxal
88 chemistry were performed at atmospheric pressure. To demonstrate the potential importance of the
89 internal pressure for atmospheric chemical reactions, this study has focused on the chemical
90 characterization of glyoxal chemistry at pressures that simulate the interior of atmospheric
91 nanoparticles (i.e., < 100 nm).

Experimental Methods

The experiments were performed using individual low-density polyethylene bags (VWR). 10 mL bulk samples were introduced into the bags, that were sealed without any air. The solutions mixtures contained 2 M ammonium sulphate ($(NH_4)_2SO_4$; (99.0%, Sigma Aldrich) and 0.25-2 M of glyoxal (40% in water, Sigma Aldrich), corresponding to a pH of 4. Experimental conditions were selected based on earlier studies which investigated the reaction of glyoxal with ammonium. Although these conditions do not mimic ambient concentrations, we selected this model system and reproduced the currently accepted conditions used in other studies and modified only the pressure at which the reaction took place. For each experiment, two sets of samples were prepared: i) "control" samples were protected from ambient light and kept at room temperature and at atmospheric pressure; ii) "pressure" samples were introduced into a high-pressure closed vessel (or reactor) and pressurized using water at 12.5, 25 or 50 MPa at room temperature (Figure S1). The 5 bags containing 4 concentrations and 1 control were pressurized in a high-pressure vessel (OC-1; High Pressure Equipment Company, Erie, Pennsylvania) by a piston screw pump (Top Industry, France). Once the piston reached the desired pressure, the high-pressure vessel was isolated (using valves) in order to obtain a stable pressure during the experiment. The pressure inside the vessel was continuously monitored and remained stable (i.e., less than 5% decrease over each experiment).

One set of samples comprises four solutions containing glyoxal (0.25, 0.5, 1 and 2M) and $(NH_4)_2SO_4$ (2M), 1 solution containing only glyoxal (2 M) and one water blank. The blanks were used to identify possible contamination from the bag itself. The results showed that the bags were not degraded by the chemicals (organics, acids, etc.) used in the experiments. The samples were maintained for 3, 6, 12, 18 and 24-h. At least three replicates for each condition (concentration, exposure time and pressure) were performed.

UV/Vis characterization. Kinetic analyses were based on measurements of the absorbance of the reaction mixtures as a function of time over 200-900 nm with a UV/Vis spectrometer (Cary 60, Agilent Technology). Directly after the end of the experiments, the samples were diluted (by a factor of 10) in deionized water to stop/significantly slow down the glyoxal reaction and ensure an optimal

quantification (i.e., peak absorbance < 1). The diluted reaction mixtures were taken and placed into 1 cm quartz cuvettes. Control experiments were performed (i.e., without dilution) to ensure that the dilution did not modify the composition of the reaction mixtures. The ratio of the peak absorbance of the solution at high pressure and at atmospheric pressure were similar with (e.g., ratio = 0.52, 2Mat 50 MPa) and without dilution (ratio = 0.56; 2M at 50 MPa). The absorption band between 260 nm and 300 nm was used to probe the formation of light-absorbing compounds produced from the reaction of glyoxal with ammonium ions. Note that using the analytical techniques employed in this study, it was not possible to directly monitor the reactants' concentrations. Therefore, no quantitative data on the thermodynamics were obtained.

Chemical characterization. Solutions exposed at atmospheric pressure and at high pressures were directly diluted (× 10,000) at the end of the experiments to stop the reaction. Diluted samples were analysed by ultra-high performance liquid chromatography (Dionex 3000, Thermo Scientific) using a Waters Acquity HSS C18 column (1.8µL, 100 x 2.1mm) coupled with a Q-Exactive Hybrid Quadrupole-Orbitrap mass spectrometer (Thermo Scientific) equipped with an electrospray ionization (ESI) source operated in negative and positive modes. The mobile phase consisted of (A) 0.1% formic acid in water (Optima® LC/MS, Fischer Scientific) and (B) 0.1% formic acid in acetonitrile (Optima® LC/MS, Fischer Scientific). Gradient elution was carried out by the A/B mixture at a total flow rate of 300 µL/min: 1% of B for 2 min, a linear gradient was used until 100% of B for 11 min, then 100% of B for 2 min and back to 1% of B in 0.1 min, and to end 1% of B for 6.9 min. Caffeine was used as an internal standard to retrieve the ionization efficiency of the different samples in order to account for the variability of the UPLC/ESI-Orbitrap. The recovery of caffeine was 86 ± 5% (1 std. dev.) and each sample was corrected for the instrumental variability.

GAMMA simulations. Calculations were performed using the photochemical box model GAMMA 5.0[25,26] to simulate the formation of light-absorbing organic material in aqueous aerosols from glyoxal following Woo et al.[27] GAMMA uses a detailed kinetic treatment of glyoxal chemistry and does not assume chemical equilibrium.[25] Gas phase concentration of glyoxal was set to 4.68×10^9 molecule cm^{-3} as previously used by Tsui et al.[26] The reaction of aqueous glyoxal with NH_4^+ to form light-absorbing organic species was simulated using the kinetics of Schwier et al.[28] for the base case and compared

with simulations where that overall rate constant was reduced to account for the effects of particle pressure following the data in Figure 3. Simulations were performed for ammonium (bi)sulfate particles at 65% RH and pH 2 with a diameter of 20, 40, 80, 160, or 320 nm, with a constant liquid water content (7.25×10^{12} cm^3cm^{-3}) and surface area density (10^{-4} cm^2cm^{-3}). No partitioning correction was applied to take into consideration the possible Kelvin effect. In other words, to evaluate the effect of the pressure, identical aqueous phase concentration of glyoxal was considered for the different size bins. A 12-hour time period (dawn to dusk) was simulated. Ambient temperature was set to vary sinusoidally through the day with a half-period of 12 h, with the minimum temperature 298.15K at dawn and dusk and maximum temperature 303.15K at midday. Photochemical rate constants were set following McNeill et al.[25]

Results and Discussion

Influence of pressure on the formation of glyoxal reaction products. Assuming a liquid particle and the known surface tension (γ) (e.g., 72.74 mN m^{-1} for water, 44.4 mN m^{-1} for SOA at 20°C),[29] the effective pressure inside nanometre-sized particles can be calculated using the Young-Laplace equation ($\Delta P = 2\gamma / r$, with r representing the radius of the particle) (Figure 1A). It should be pointed out the surface tension of nanoparticles remains basically unknown and only the surface tension of large aerosols can be determined. Hence, surface tension of alpha-pinene-derived SOA and pure water were selected as lower and upper limits, respectively, to probe the impact of the pressure. Indeed, earlier studies have shown that atmospherically relevant particles, including inorganic and organic species, have surface tension within this range.[29–33] Besides surface tension, other parameters can influence the pressure, such as the phase state and/or chemical composition of the particles. For example, the surface tension of dissolved SOA from the oxidation of biogenic compounds can be reduced by a factor of two compared to pure water.[29] According to various studies, biogenic SOA particles produced in laboratory chambers or observed in the ambient atmosphere may exist in various solid and liquid forms.[34–36] However, nanometre-sized organic aerosols remain liquid under most environmental conditions.[36–38] To investigate the impact of pressure on atmospheric chemical reactions that occur within the particles, we studied the reaction between glyoxal and ammonium sulphate under

different pressures ranging from 1 atm to 500 atm: 0.1, 12.5, 25 and 50 MPa, corresponding to coarse particles and to fine aerosol particles of 23, 12 and 6 nm in diameter, respectively (diameters calculated assuming a liquid droplet with a surface tension of pure water). As previously reported, products formed from the glyoxal-ammonium sulphate reaction absorb light in the UV and visible wavelengths providing a convenient way to follow the reaction (Figures 1 and S1-S4).[19,20,39] Figure 1B shows the time evolution of the UV absorption spectra of a solution initially containing 0.25, 0.5, 1 and 2 M glyoxal mixed with 2 M of ammonium sulphate ($(NH_4)_2SO_4$) up to 24 hours, corresponding to experimental conditions conducted under atmospheric pressure (i.e., 1 atm internal pressure).[20] The resulting solution is weakly acidic (pH ~ 4), thus simulating aqueous tropospheric aerosol particles. The absorbance of solutions at atmospheric pressure increased with time. Under high pressures, a significant decrease in the total absorbance is observed for all conditions investigated in this study (Figures 1C & 1D; S2). Already after 3h, the difference between experiments conducted at atmospheric pressure and 50 MPa experiments is significant (i.e., $Abs_{P50}/Abs_{P0.1} = 0.66 \pm 0.02$) underlying the impact of increased pressure on the rate of glyoxal's reaction under slightly acidic aqueous conditions. Interestingly, related reactions between carbonyls and amines have been studied in the context of food science and a retarding effect of high (400 MPa) pressure was demonstrated. [40–42] This observation is consistent with our results, although we find an effect on the reaction of glyoxal with ammonium sulphate at much milder pressures e.g., a slowing down by a factor of 2 at 25 MPa. This proves that pressure can already have a pronounced effect in a relevant size range for atmospheric aerosols. It is important to point out that in this study we have explored the effect of the pressure in bulk solution in a closed system, i.e., no partitioning was considered. As a result, the decreasing rate constant is only due to the effect of the pressure on the chemical processes. Additional studies are required to relate what we observed in bulk solution to aerosol particles.

Ultra-performance liquid chromatography coupled with hybrid quadrupole Orbitrap mass spectrometry analysis, performed in negative and positive modes, shows the presence of a wide variety of reaction products (Figure 2A). The major reaction products, detected by their protonated ions and consistent with other studies that form through the iminum pathway,[19,20,22,24,43] (i.e., imidazole ($C_3H_5N_2^+$), imidazole-2-carboxaldehyde ($C_4H_5ON_2^+$), hydrated imidazole-2-carboxaldehyde

($C_4H_7O_2N_2^+$)), are observed in all the experiments. This product distribution is consistent with the existing literature, where high-molecular-weight organic compounds, formed by accretion reactions, have been observed.[12,19,20,43] Although the reaction products are similar in our study, samples exposed to high pressures exhibit much lower product yields compared to the atmospheric pressure samples (Figure 2A). More specifically, concentrations of the primary products, such as imidazole, reduced by a factor of 2 after 24 hours, further highlighting the impact of pressure on this chemical system (Figure 2B). As in the Maillard reaction,[41,44] chemical processes leading to the formation of such products increase the volume of reaction (i.e., $\Delta V > 0$). Therefore, at higher pressure, the product formation is reduced. In addition, formation of N-containing oligomers is also significantly supressed by the pressure (~ 40% after 24h). For example, the formation of $C_6H_{10}O_6N^+$ dimer is strongly reduced under high pressures (Figure 2). Finally, it is noted that the glyoxal products formed from aldol/acetal oligomerization were not observed in either the atmospheric pressure or the high-pressure samples. Overall, the results obtained in this study reveal that the Laplace pressure, i.e., the pressure within atmospheric particles, can strongly influence the multiphase processes involved in the formation and growth of SOA.

Particle size-dependence kinetics. As the light-absorbing compounds absorb light at 290 nm (Figure S3), monitoring the evolution of this absorbance band provides insight into the overall kinetics of the reaction between glyoxal and ammonium cations. The reactions are first order (Figure S4) within the first 24 hours, which is consistent with an earlier study.[20] Therefore, for each set of experiments (i.e., four concentrations at a given pressure and four concentrations at atmospheric pressure), where each condition was repeated at least three times, a global rate constant (k_{obs}) can be obtained. As shown in Figure 3A, a pressure-dependent rate constant is determined, using the average k_{obs} determined for each pressure. Using linear regression, particle size-dependence of the rate constant can be obtained, as shown in Figure 3B. Two surface tension values were selected to obtain the rate constant as a function of particle size: the surface tension of water (72.74 mN m^{-1}), which represents an upper limit, and the surface tension of α-pinene SOA, which is formed under humid conditions (44.4 mN m^{-1}).[29] α-pinene-derived SOA is used as model SOA because monoterpenes are among the most important

SOA precursors on a global scale.[45,46] Therefore, for ultrafine particles, i.e., < 100 nm, the reduction of glyoxal chemistry is important, indicating that chemical processes identical or similar to those involved in the heterogeneous chemistry of the dicarbonyls, can be strongly reduced in ultrafine atmospheric aerosols.

To further illustrate particle size-dependence chemistry, the photochemical box model GAMMA was used to simulate imidazole formation as a function of particle size (and hence pressure), The calculations were performed in discrete size bins (i.e., 20, 40, 80, 160, and 320 nm), for 12 hours (Figure 4).[25,27,47] The simulations show that the pressure effect on the formation of imidazole and other brown carbon species is negligible, for the largest size bin (i.e., 320 nm). However, the heterogeneous process is greatly reduced when the pressure within the nanometre-sized particles increases. For example, the formation of glyoxal reaction products is reduced by 20% for the smallest size bin (i.e., 20 nm). This further underlines that chemical processes that are expected to grow ultrafine particles[48] are likely to be strongly influenced by their high internal pressure.

By studying an important chemical reaction under relevant atmospheric conditions, we showed that the high pressure inside nanometre-sized aerosol particles is a key property that has not been considered hitherto and that can have a significant influence on the chemical processes governing atmospheric particle growth and evolution. More importantly we demonstrated that pressures can have a noticeable effect at much milder pressures (~ 1-2 order of magnitude lower) than has been studied before. Such pressures are highly relevant for atmospheric aerosols. However, it is important to note that due to the relative short lifetime of nanoparticles (i.e., from a few hours to a day), the pressure would have a noticeable effect for chemical reactions that are greatly impacted by the Laplace pressure with rate constant comparable or shorter than the aerosol lifetime. Considering the Evans-Polanyi principle, Le Noble and co-workers[49] have derived a function to represent the reaction profile for a one-step reaction. By using such an approach, it is possible to evaluate the impact of the pressure on changes in the transition state. As we studied a global reaction, it was not possible to isolate a single reaction step using the analytical techniques employed by Le Noble et al.[49] However, based on the existing literature we can derive some information providing hints that identify which reaction step may have been mostly impacted by the pressure.[8,50] For example, the breaking of bonds within a

reaction mechanism involves the separation of atoms from each other from covalent distances to van der Waals distances. In fact, the transformation of NH_4^+ to H^+ and NH_3, which was identified to be a key state of the investigated chemistry,[19,24] is known to be hindered by pressure (i.e., $\Delta V = 7$ cm^3 mol^{-1})[50,51], and might explain the observation made here. While we found a negative effect here for this specific reaction on the formation and growth of SOA, other potentially important particle phase reactions, especially those with negative reaction volumes and/or negative activation volumes, could be strongly promoted by pressure.[1,22] The extensive literature on the effects of pressure on organic and inorganic chemical reactions in solutions strongly suggests that several types of atmospheric reactions could also be influenced by pressure.[8] For example, nucleophilic substitution reactions of various types of organic compounds at high pressure are favoured because ionisation reactions in the transition state of the reaction cause negative activation volumes. While the experiments performed in this work show a clear impact of the pressure, additional experiments using aerosol droplets are required to further confirm the results presented here. Indeed, interfacial chemistry, gas-liquid exchanges i.e., processes not considered here, may also be affected by the pressure in addition to the "bulk" chemical reaction kinetics and equilibria. Overall, our results provide information about the potentially critical influence of pressure on the chemistry occurring within atmospheric nanoparticles. While such processes have not been reported before, this work emphasizes the need to consider particle phase processing under atmospherically relevant conditions.

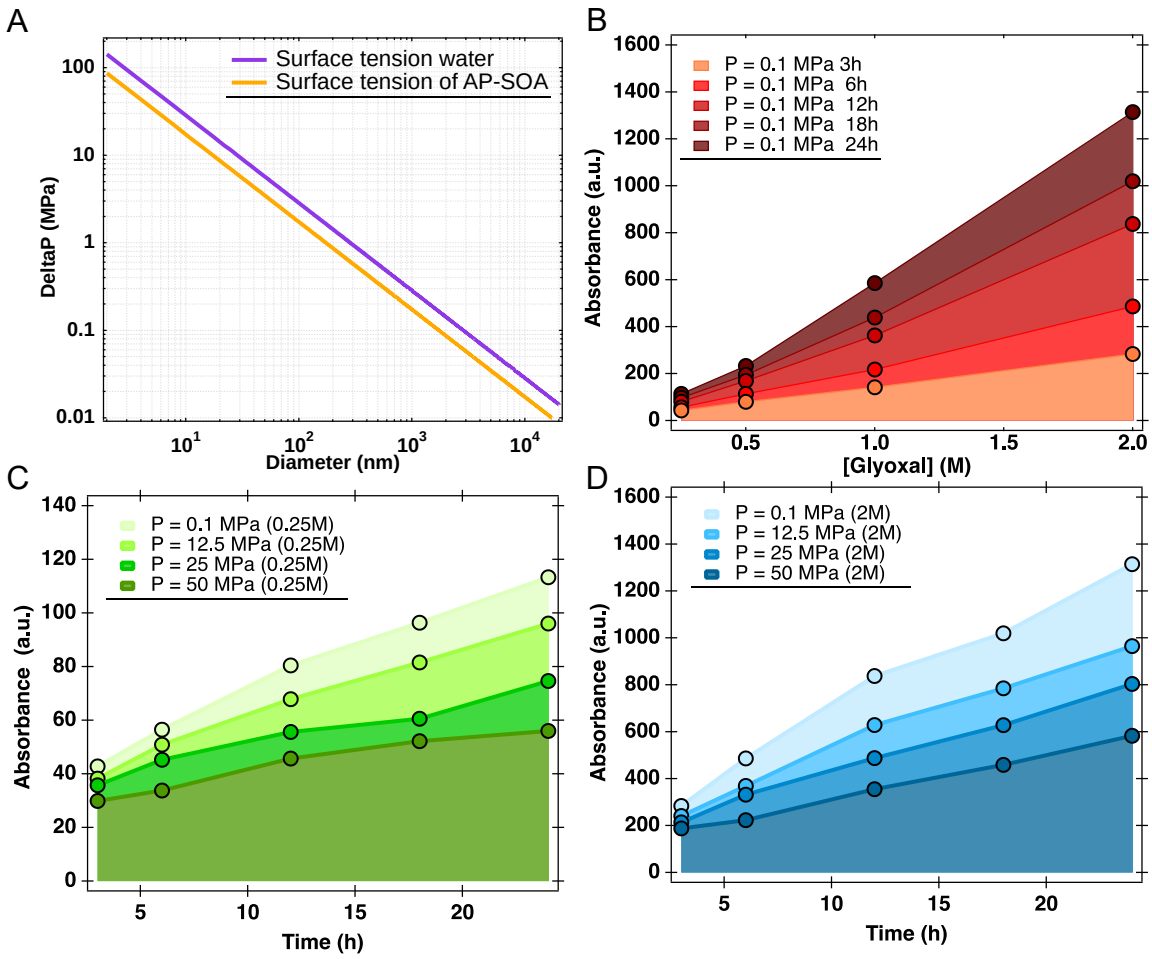

Figure 1. (A) Pressure inside 2 to 1000 nm aerosol particles with surface tension of water and α-pinene SOA. (B) Evolution of the absorbance (non-cumulative) of light-absorbing glyoxal reaction products at different reaction time and as function of glyoxal concentration. Non-cumulative absorbance of light-absorbing glyoxal reaction products at different pressures of (C) 0.25 M glyoxal/ 2 M AS and (D) 2 M glyoxal/ 2 M AS as a function of reaction time.

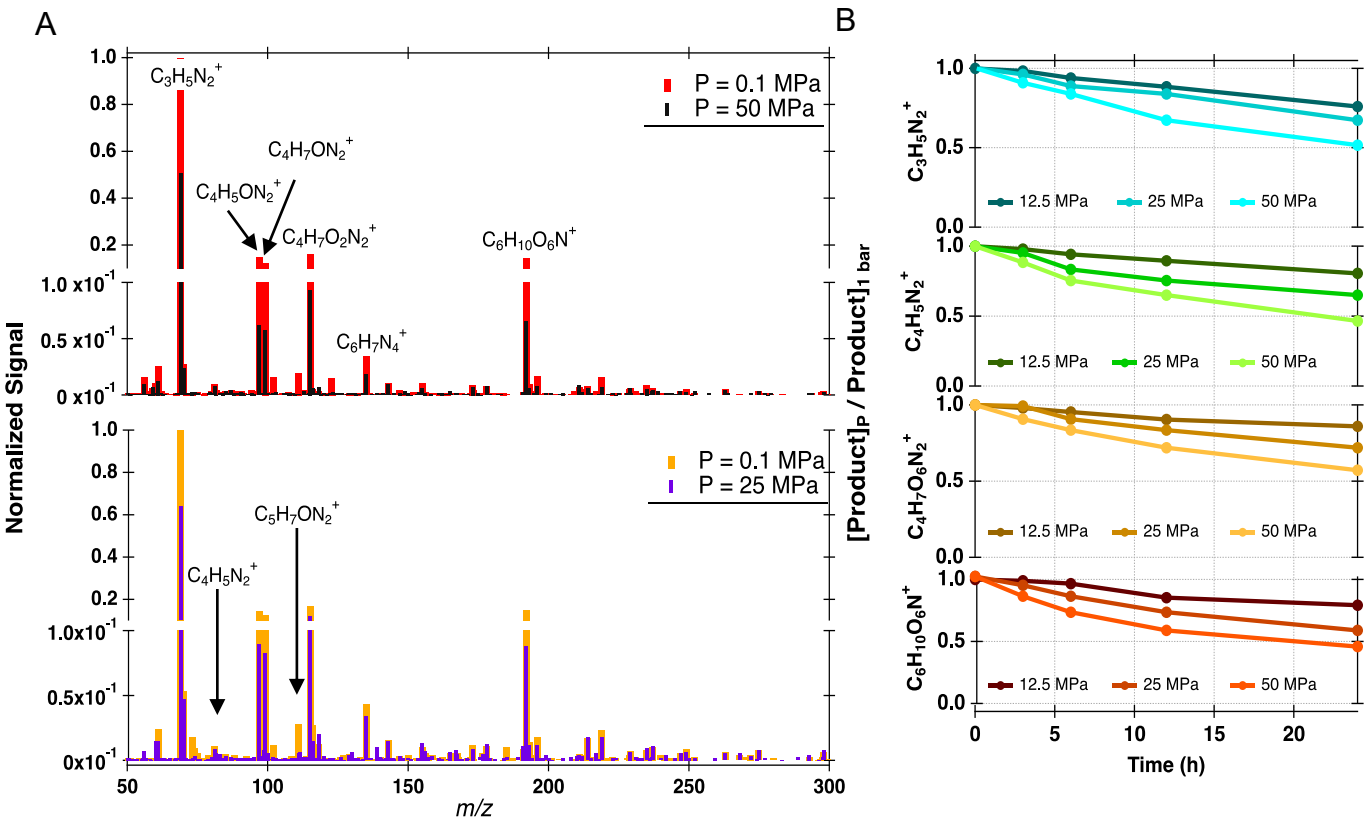

283 **Figure 2.** (A) Impact of the pressure on the chemical composition of organic products from the reaction
284 of glyoxal with ammonium sulphate measured by UPLC-(+)ESI-Orbitrap. Mass spectra were averaged
285 across the chromatogram and background subtracted (i.e., water samples served as blank). (B) Evolution
286 of the relative concentration ($[Product]_{P>>1\ atm}$ / $[Product]_{P=1atm}$) of the main reaction products as a
287 function of time.
288

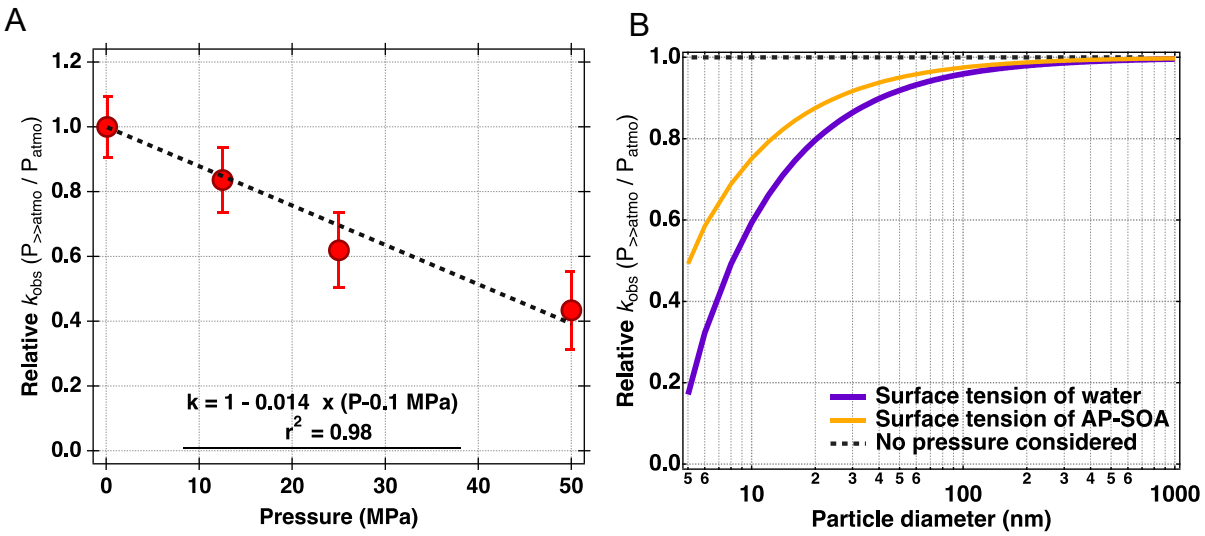

289

290 **Figure 3.** (A) Relative glyoxal/AS reaction rate constant of light-absorbing product formation as a
291 function of pressure. The overall uncertainty of the relative rate constant is 0.074 (one standard
292 deviation). (B) Relative glyoxal/AS reaction rate constant as a function of aerosol particle diameter
293 considering different aerosol surface tension.

294

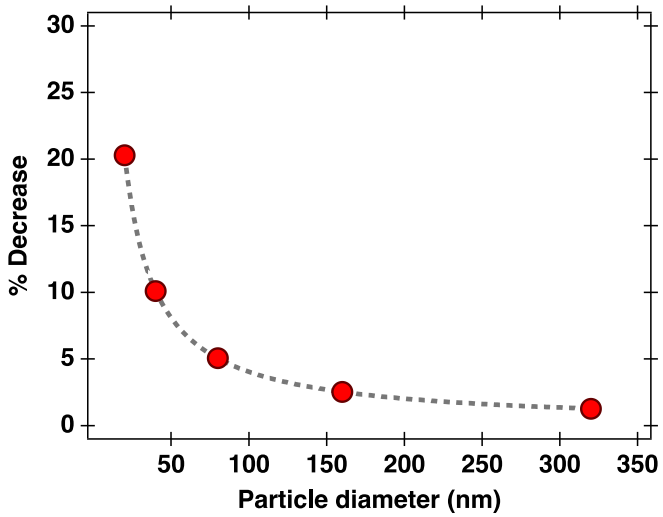

295

296 **Figure 4.** Decrease of the formation of glyoxal reaction products as a function of particle size

297 diameter. Simulations were performed using GAMMA for different size bins diameters (e.g., 20, 40,

298 80, 160, and 320 nm) and under Eastern US rural conditions.

ASSOCIATED CONTENT

Figure S1 shows the absorbance of light-absorbing glyoxal oxidation products at different reaction time and pressure. Figure S2 displays the relative absorbance of light-absorbing glyoxal oxidation products under the different experimental conditions used in this study. Figure S3 shows the absorption spectra of glyoxal products after 24 hours. Figure S4 shows the first-order kinetic fit for the different experiments performed in this study. This material is available free of charge via the Internet at http://pubs.acs.org/.

AUTHOR INFORMATION

Corresponding Author

*E-mail (M. R.): matthieu.riva@ircelyon.univ-lyon1.fr
*E-mail (T. H.): t.hoffmann@uni-mainz.de
*E-mail (C. G.): christian.george@ircelyon.univ-lyon1.fr

Funding Sources

This work is funded in part by the European Research Council (ERC-StG MAARvEL, grant nr 852161), and by the Deutsche Forschungsgemeinschaft (DFG, HO 1748/19-1)

ACKNOWLEDGMENT

The authors wish to thank the European Research Council (ERC-StG), the Deutsche Forschungsgemeinschaft and the University of Lyon for financial support. S.A.N. thanks the Université Claude Bernard Lyon 1 for providing him with a visiting professorship in the summer of 2018.

ASSOCIATED CONTENT

Figure S1 shows the experimental device (high-pressure vessel) used in this study. This material is available free of charge via the Internet at http://pubs.acs.org/.

References

(1) Hallquist, M.; Wenger, J. C.; Baltensperger, U.; Rudich, Y.; Simpson, D.; Claeys, M.; Dommen, J.; Donahue, N. M.; George, C.; Goldstein, A. H.; Hamilton, J. F.; Herrmann, H.; Hoffmann, T.; Iinuma, Y.; Jang, M.; Jenkin, M. E.; Jimenez, J. L.; Kiendler-Scharr, A.; Maenhaut, W.; McFiggans, G.; Mentel, Th. F.; Monod, A.; Prévôt, A. S. H.; Seinfeld, J. H.; Surratt, J. D.; Szmigielski, R.; Wildt, J. The Formation, Properties and Impact of Secondary Organic Aerosol: Current and Emerging Issues. *Atmospheric Chemistry and Physics* **2009**, *9* (14), 5155–5236. https://doi.org/10.5194/acp-9-5155-2009.

(2) Albrecht, B. A. Aerosols, Cloud Microphysics, and Fractional Cloudiness. *Science* **1989**, *245* (4923), 1227–1230. https://doi.org/10.1126/science.245.4923.1227.

(3) Twomey, S. The Influence of Pollution on the Shortwave Albedo of Clouds. *Journal of the Atmospheric Sciences* **1977**, *34* (7), 1149–1152. https://doi.org/10.1175/1520-0469(1977)034<1149:TIOPOT>2.0.CO;2.

(4) Gakidou, E.; Afshin, A.; Abajobir, A. A.; Abate, K. H.; Abbafati, C.; Abbas, K. M.; Abd-Allah, F.; Abdulle, A. M.; Abera, S. F.; Aboyans, V.; Abu-Raddad, L. J.; Abu-Rmeileh, N. M. E.; Abyu, G. Y.; Adedeji, I. A.; Adetokunboh, O.; Afarideh, M.; Agrawal, A.; Agrawal, S.; Ahmadieh, H.; Ahmed, M. B.; Aichour, M. T. E.; Aichour, A. N.; Aichour, I.; Akinyemi, R. O.; Akseer, N.; Alahdab, F.; Al-Aly, Z.; Alam, K.; Alam, N.; Alam, T.; Alasfoor, D.; Alene, K. A.; Ali, K.; Alizadeh-Navaei, R.; Alkerwi, A.; Alla, F.; Allebeck, P.; Al-Raddadi, R.; Alsharif, U.; Altirkawi, K. A.; Alvis-Guzman, N.; Amare, A. T.; Amini, E.; Ammar, W.; Amoako, Y. A.; Ansari, H.; Antó, J. M.; Antonio, C. A. T.; Anwari, P.; Arian, N.; Ärnlöv, J.; Artaman, A.; Aryal, K. K.; Asayesh, H.; Asgedom, S. W.; Atey, T. M.; Avila-Burgos, L.; Avokpaho, E. F. G. A.; Awasthi, A.; Azzopardi, P.; Bacha, U.; Badawi, A.; Balakrishnan, K.; Ballew, S. H.; Barac, A.; Barber, R. M.; Barker-Collo, S. L.; Bärnighausen, T.; Barquera, S.; Barregard, L.; Barrero, L. H.; Batis, C.; Battle, K. E.; Baumgarner, B. R.; Baune, B. T.; Beardsley, J.; Bedi, N.; Beghi, E.; Bell, M. L.; Bennett, D. A.; Bennett, J. R.; Bensenor, I. M.; Berhane, A.; Berhe, D. F.; Bernabé, E.; Betsu, B. D.; Beuran, M.; Beyene, A. S.; Bhansali, A.; Bhutta, Z. A.; Bicer, B. K.; Bikbov, B.; Birungi, C.; Biryukov, S.; Blosser, C. D.; Boneya, D. J.; Bou-Orm, I. R.; Brauer, M.; Breitborde, N. J. K.; Brenner, H.; Brugha, T. S.; Bulto, L. N. B.; Butt, Z. A.; Cahuana-Hurtado, L.; Cárdenas, R.; Carrero, J. J.; Castañeda-Orjuela, C. A.; Catalá-López, F.; Cercy, K.; Chang, H.-Y.; Charlson, F. J.; Chimed-Ochir, O.; Chisumpa, V. H.; Chitheer, A. A.; Christensen, H.; Christopher, D. J.; Cirillo, M.; Cohen, A. J.; Comfort, H.; Cooper, C.; Coresh, J.; Cornaby, L.; Cortesi, P. A.; Criqui, M. H.; Crump, J. A.; Dandona, L.; Dandona, R.; das Neves, J.; Davey, G.; Davitoiu, D. V.; Davletov, K.; de Courten, B.; Defo, B. K.; Degenhardt, L.; Deiparine, S.; Dellavalle, R. P.; Deribe, K.; Deshpande, A.; Dharmaratne, S. D.; Ding, E. L.; Djalalinia, S.; Do, H. P.; Dokova, K.; Doku, D. T.; Donkelaar, A. van; Dorsey, E. R.; Driscoll, T. R.; Dubey, M.; Duncan, B. B.; Duncan, S.; Ebrahimi, H.; El-Khatib, Z. Z.; Enayati, A.; Endries, A. Y.; Ermakov, S. P.; Erskine, H. E.; Eshrati, B.; Eskandarieh, S.; Esteghamati, A.; Estep, K.; Faraon, E. J. A.; Farinha, C. S. e S.; Faro, A.; Farzadfar, F.; Fay, K.; Feigin, V. L.; Fereshtehnejad, S.-M.; Fernandes, J. C.; Ferrari, A. J.; Feyissa, T. R.; Filip, I.; Fischer, F.; Fitzmaurice, C.; Flaxman, A. D.; Foigt, N.; Foreman, K. J.; Frostad, J. J.; Fullman, N.; Fürst, T.; Furtado, J. M.; Ganji, M.; Garcia-Basteiro, A. L.; Gebrehiwot, T. T.; Geleijnse, J. M.; Geleto, A.; Gemechu, B. L.; Gesesew, H. A.; Gething, P. W.; Ghajar, A.; Gibney, K. B.; Gill, P. S.; Gillum, R. F.; Giref, A. Z.; Gishu, M. D.; Giussani, G.; Godwin, W. W.; Gona, P. N.; Goodridge, A.; Gopalani, S. V.; Goryakin, Y.; Goulart, A. C.; Graetz, N.; Gugnani, H. C.; Guo, J.; Gupta, R.; Gupta, T.; Gupta, V.; Gutiérrez, R. A.; Hachinski, V.; Hafezi-Nejad, N.; Hailu, G. B.; Hamadeh, R. R.; Hamidi, S.; Hammami, M.; Handal, A. J.; Hankey, G. J.; Hanson, S. W.; Harb, H. L.; Hareri, H. A.; Hassanvand, M. S.; Havmoeller, R.; Hawley, C.; Hay, S. I.; Hedayati, M. T.; Hendrie, D.; Heredia-Pi, I. B.; Hernandez, J. C. M.; Hoek, H. W.; Horita, N.; Hosgood, H. D.; Hostiuc, S.; Hoy, D. G.; Hsairi, M.; Hu, G.; Huang, J. J.; Huang, H.; Ibrahim, N. M.; Iburg, K. M.; Ikeda, C.; Inoue, M.; Irvine, C. M. S.; Jackson, M. D.; Jacobsen, K. H.; Jahanmehr, N.; Jakovljevic, M. B.; Jauregui, A.; Javanbakht, M.; Jeemon, P.; Johansson, L. R. K.; Johnson, C. O.; Jonas, J. B.; Jürisson, M.; Kabir, Z.; Kadel, R.; Kahsay, A.; Kamal, R.; Karch, A.; Karema, C. K.; Kasaeian, A.; Kassebaum, N. J.; Kastor, A.; Katikireddi, S. V.; Kawakami, N.; Keiyoro, P. N.; Kelbore, S. G.; Kemmer, L.; Kengne, A. P.; Kesavachandran, C. N.; Khader, Y. S.; Khalil, I. A.; Khan, E. A.; Khang, Y.-H.; Khosravi, A.; Khubchandani, J.; Kiadaliri, A. A.; Kieling,

C.; Kim, J. Y.; Kim, Y. J.; Kim, D.; Kimokoti, R. W.; Kinfu, Y.; Kisa, A.; Kissimova-Skarbek, K. A.; Kivimaki, M.; Knibbs, L. D.; Knudsen, A. K.; Kopec, J. A.; Kosen, S.; Koul, P. A.; Koyanagi, A.; Kravchenko, M.; Krohn, K. J.; Kromhout, H.; Kumar, G. A.; Kutz, M.; Kyu, H. H.; Lal, D. K.; Lalloo, R.; Lallukka, T.; Lan, Q.; Lansingh, V. C.; Larsson, A.; Lee, P. H.; Lee, A.; Leigh, J.; Leung, J.; Levi, M.; Levy, T. S.; Li, Y.; Li, Y.; Liang, X.; Liben, M. L.; Linn, S.; Liu, P.; Lodha, R.; Logroscino, G.; Looker, K. J.; Lopez, A. D.; Lorkowski, S.; Lotufo, P. A.; Lozano, R.; Lunevicius, R.; Macarayan, E. R. K.; Magdy Abd El Razek, H.; Magdy Abd El Razek, M.; Majdan, M.; Majdzadeh, R.; Majeed, A.; Malekzadeh, R.; Malhotra, R.; Malta, D. C.; Mamun, A. A.; Manguerra, H.; Mantovani, L. G.; Mapoma, C. C.; Martin, R. V.; Martinez-Raga, J.; Martins-Melo, F. R.; Mathur, M. R.; Matsushita, K.; Matzopoulos, R.; Mazidi, M.; McAlinden, C.; McGrath, J. J.; Mehata, S.; Mehndiratta, M. M.; Meier, T.; Melaku, Y. A.; Memiah, P.; Memish, Z. A.; Mendoza, W.; Mengesha, M. M.; Mensah, G. A.; Mensink, G. B. M.; Mereta, S. T.; Meretoja, T. J.; Meretoja, A.; Mezgebe, H. B.; Micha, R.; Millear, A.; Miller, T. R.; Minnig, S.; Mirarefin, M.; Mirrakhimov, E. M.; Misganaw, A.; Mishra, S. R.; Mohammad, K. A.; Mohammed, K. E.; Mohammed, S.; Mohan, M. B. V.; Mokdad, A. H.; Monasta, L.; Montico, M.; Moradi-Lakeh, M.; Moraga, P.; Morawska, L.; Morrison, S. D.; Mountjoy-Venning, C.; Mueller, U. O.; Mullany, E. C.; Muller, K.; Murthy, G. V. S.; Musa, K. I.; Naghavi, M.; Naheed, A.; Nangia, V.; Natarajan, G.; Negoi, R. I.; Negoi, I.; Nguyen, C. T.; Nguyen, Q. L.; Nguyen, T. H.; Nguyen, G.; Nguyen, M.; Nichols, E.; Ningrum, D. N. A.; Nomura, M.; Nong, V. M.; Norheim, O. F.; Norrving, B.; Noubiap, J. J. N.; Obermeyer, C. M.; Ogbo, F. A.; Oh, I.-H.; Oladimeji, O.; Olagunju, A. T.; Olagunju, T. O.; Olivares, P. R.; Olsen, H. E.; Olusanya, B. O.; Olusanya, J. O.; Opio, J. N.; Oren, E.; Ortiz, A.; Ota, E.; Owolabi, M. O.; Pa, M.; Pacella, R. E.; Pana, A.; Panda, B. K.; Panda-Jonas, S.; Pandian, J. D.; Papachristou, C.; Park, E.-K.; Parry, C. D.; Patten, S. B.; Patton, G. C.; Pereira, D. M.; Perico, N.; Pesudovs, K.; Petzold, M.; Phillips, M. R.; Pillay, J. D.; Piradov, M. A.; Pishgar, F.; Plass, D.; Pletcher, M. A.; Polinder, S.; Popova, S.; Poulton, R. G.; Pourmalek, F.; Prasad, N.; Purcell, C.; Qorbani, M.; Radfar, A.; Rafay, A.; Rahimi-Movaghar, A.; Rahimi-Movaghar, V.; Rahman, M. H. U.; Rahman, M. A.; Rahman, M.; Rai, R. K.; Rajsic, S.; Ram, U.; Rawaf, S.; Rehm, C. D.; Rehm, J.; Reiner, R. C.; Reitsma, M. B.; Remuzzi, G.; Renzaho, A. M. N.; Resnikoff, S.; Reynales-Shigematsu, L. M.; Rezaei, S.; Ribeiro, A. L.; Rivera, J. A.; Roba, K. T.; Rojas-Rueda, D.; Roman, Y.; Room, R.; Roshandel, G.; Roth, G. A.; Rothenbacher, D.; Rubagotti, E.; Rushton, L.; Sadat, N.; Safdarian, M.; Safi, S.; Safiri, S.; Sahathevan, R.; Salama, J.; Salomon, J. A.; Samy, A. M.; Sanabria, J. R.; Sanchez-Niño, M. D.; Sánchez-Pimienta, T. G.; Santomauro, D.; Santos, I. S.; Santric Milicevic, M. M.; Sartorius, B.; Satpathy, M.; Sawhney, M.; Saxena, S.; Schmidt, M. I.; Schneider, I. J. C.; Schutte, A. E.; Schwebel, D. C.; Schwendicke, F.; Seedat, S.; Sepanlou, S. G.; Serdar, B.; Servan-Mori, E. E.; Shaddick, G.; Shaheen, A.; Shahraz, S.; Shaikh, M. A.; Shamsipour, M.; Shamsizadeh, M.; Shariful Islam, S. M.; Sharma, J.; Sharma, R.; She, J.; Shen, J.; Shi, P.; Shibuya, K.; Shields, C.; Shiferaw, M. S.; Shigematsu, M.; Shin, M.-J.; Shiri, R.; Shirkoohi, R.; Shishani, K.; Shoman, H.; Shrime, M. G.; Sigfusdottir, I. D.; Silva, D. A. S.; Silva, J. P.; Silveira, D. G. A.; Singh, J. A.; Singh, V.; Sinha, D. N.; Skiadaresi, E.; Slepak, E. L.; Smith, D. L.; Smith, M.; Sobaih, B. H. A.; Sobngwi, E.; Soneji, S.; Sorensen, R. J. D.; Sposato, L. A.; Sreeramareddy, C. T.; Srinivasan, V.; Steel, N.; Stein, D. J.; Steiner, C.; Steinke, S.; Stokes, M. A.; Strub, B.; Subart, M.; Sufiyan, M. B.; Suliankatchi, R. A.; Sur, P. J.; Swaminathan, S.; Sykes, B. L.; Szoeke, C. E. I.; Tabarés-Seisdedos, R.; Tadakamadla, S. K.; Takahashi, K.; Takala, J. S.; Tandon, N.; Tanner, M.; Tarekegn, Y. L.; Tavakkoli, M.; Tegegne, T. K.; Tehrani-Banihashemi, A.; Terkawi, A. S.; Tesssema, B.; Thakur, J.; Thamsuwan, O.; Thankappan, K. R.; Theis, A. M.; Thomas, M. L.; Thomson, A. J.; Thrift, A. G.; Tillmann, T.; Tobe-Gai, R.; Tobollik, M.; Tollanes, M. C.; Tonelli, M.; Topor-Madry, R.; Torre, A.; Tortajada, M.; Touvier, M.; Tran, B. X.; Truelsen, T.; Tuem, K. B.; Tuzcu, E. M.; Tyrovolas, S.; Ukwaja, K. N.; Uneke, C. J.; Updike, R.; Uthman, O. A.; van Boven, J. F. M.; Varughese, S.; Vasankari, T.; Veerman, L. J.; Venkateswaran, V.; Venketasubramanian, N.; Violante, F. S.; Vladimirov, S. K.; Vlassov, V. V.; Vollset, S. E.; Vos, T.; Wadilo, F.; Wakayo, T.; Wallin, M. T.; Wang, Y.-P.; Weichenthal, S.; Weiderpass, E.; Weintraub, R. G.; Weiss, D. J.; Werdecker, A.; Westerman, R.; Whiteford, H. A.; Wiysonge, C. S.; Woldeyes, B. G.; Wolfe, C. D. A.; Woodbrook, R.; Workicho, A.; Xavier, D.; Xu, G.; Yadgir, S.; Yakob, B.; Yan, L. L.; Yaseri, M.; Yimam, H. H.; Yip, P.; Yonemoto, N.; Yoon, S.-J.; Yotebieng, M.; Younis, M. Z.; Zaidi, Z.; Zaki, M. E. S.; Zavala-Arciniega, L.; Zhang, X.; Zimsen, S. R. M.; Zipkin, B.; Zodpey, S.; Lim, S. S.; Murray, C. J. L. Global, Regional, and National Comparative Risk Assessment of 84 Behavioural, Environmental and

Occupational, and Metabolic Risks or Clusters of Risks, 1990–2016: A Systematic Analysis for the Global Burden of Disease Study 2016. *The Lancet* **2017**, *390* (10100), 1345–1422. https://doi.org/10.1016/S0140-6736(17)32366-8.
(5) Shrivastava, M.; Cappa, C. D.; Fan, J.; Goldstein, A. H.; Guenther, A. B.; Jimenez, J. L.; Kuang, C.; Laskin, A.; Martin, S. T.; Ng, N. L.; Petaja, T.; Pierce, J. R.; Rasch, P. J.; Roldin, P.; Seinfeld, J. H.; Shilling, J.; Smith, J. N.; Thornton, J. A.; Volkamer, R.; Wang, J.; Worsnop, D. R.; Zaveri, R. A.; Zelenyuk, A.; Zhang, Q. Recent Advances in Understanding Secondary Organic Aerosol: Implications for Global Climate Forcing: Advances in Secondary Organic Aerosol. *Reviews of Geophysics* **2017**, *55* (2), 509–559. https://doi.org/10.1002/2016RG000540.
(6) Jimenez, J. L.; Canagaratna, M. R.; Donahue, N. M.; Prevot, A. S. H.; Zhang, Q.; Kroll, J. H.; DeCarlo, P. F.; Allan, J. D.; Coe, H.; Ng, N. L.; Aiken, A. C.; Docherty, K. S.; Ulbrich, I. M.; Grieshop, A. P.; Robinson, A. L.; Duplissy, J.; Smith, J. D.; Wilson, K. R.; Lanz, V. A.; Hueglin, C.; Sun, Y. L.; Tian, J.; Laaksonen, A.; Raatikainen, T.; Rautiainen, J.; Vaattovaara, P.; Ehn, M.; Kulmala, M.; Tomlinson, J. M.; Collins, D. R.; Cubison, M. J.; E.; Dunlea, J.; Huffman, J. A.; Onasch, T. B.; Alfarra, M. R.; Williams, P. I.; Bower, K.; Kondo, Y.; Schneider, J.; Drewnick, F.; Borrmann, S.; Weimer, S.; Demerjian, K.; Salcedo, D.; Cottrell, L.; Griffin, R.; Takami, A.; Miyoshi, T.; Hatakeyama, S.; Shimono, A.; Sun, J. Y.; Zhang, Y. M.; Dzepina, K.; Kimmel, J. R.; Sueper, D.; Jayne, J. T.; Herndon, S. C.; Trimborn, A. M.; Williams, L. R.; Wood, E. C.; Middlebrook, A. M.; Kolb, C. E.; Baltensperger, U.; Worsnop, D. R. Evolution of Organic Aerosols in the Atmosphere. *Science* **2009**, *326* (5959), 1525–1529. https://doi.org/10.1126/science.1180353.
(7) Ibach, H. *Physics of Surfaces and Interfaces*; Springer: Berlin; New York, 2006.
(8) Drljaca, A.; Hubbard, C. D.; van Eldik, R.; Asano, T.; Basilevsky, M. V.; le Noble, W. J. Activation and Reaction Volumes in Solution. 3. *Chemical Reviews* **1998**, *98* (6), 2167–2290. https://doi.org/10.1021/cr970461b.
(9) Laidler, K. J.; King, M. C. Development of Transition-State Theory. *J. Phys. Chem.* **1983**, *87* (15), 2657–2664. https://doi.org/10.1021/j100238a002.
(10) Chen, B.; Hoffmann, R.; Cammi, R. The Effect of Pressure on Organic Reactions in Fluids-a New Theoretical Perspective. *Angew. Chem. Int. Ed.* **2017**, *56* (37), 11126–11142. https://doi.org/10.1002/anie.201705427.
(11) Fu, T.-M.; Jacob, D. J.; Wittrock, F.; Burrows, J. P.; Vrekoussis, M.; Henze, D. K. Global Budgets of Atmospheric Glyoxal and Methylglyoxal, and Implications for Formation of Secondary Organic Aerosols. *Journal of Geophysical Research* **2008**, *113* (D15). https://doi.org/10.1029/2007JD009505.
(12) Galloway, M. M.; Chhabra, P. S.; Chan, A. W. H.; Surratt, J. D.; Flagan, R. C.; Seinfeld, J. H.; Keutsch, F. N. Glyoxal Uptake on Ammonium Sulphate Seed Aerosol: Reaction Products and Reversibility of Uptake under Dark and Irradiated Conditions. *Atmos. Chem. Phys.* **2009**, *9* (10), 3331–3345. https://doi.org/10.5194/acp-9-3331-2009.
(13) Liggio, J. Reactive Uptake of Glyoxal by Particulate Matter. *J. Geophys. Res.* **2005**, *110* (D10), D10304. https://doi.org/10.1029/2004JD005113.
(14) Kroll, J. H.; Ng, N. L.; Murphy, S. M.; Varutbangkul, V.; Flagan, R. C.; Seinfeld, J. H. Chamber Studies of Secondary Organic Aerosol Growth by Reactive Uptake of Simple Carbonyl Compounds. *J. Geophys. Res.* **2005**, *110* (D23), D23207. https://doi.org/10.1029/2005JD006004.
(15) Corrigan, A. L.; Hanley, S. W.; De Haan, D. O. Uptake of Glyoxal by Organic and Inorganic Aerosol. *Environ. Sci. Technol.* **2008**, *42* (12), 4428–4433. https://doi.org/10.1021/es7032394.
(16) Haan, D. O. D.; Corrigan, A. L.; Smith, K. W.; Stroik, D. R.; Turley, J. J.; Lee, F. E.; Tolbert, M. A.; Jimenez, J. L.; Cordova, K. E.; Ferrell, G. R. Secondary Organic Aerosol-Forming Reactions of Glyoxal with Amino Acids. *Environ. Sci. Technol.* **2009**, *43* (8), 2818–2824. https://doi.org/10.1021/es803534f.
(17) Ervens, B.; Volkamer, R. Glyoxal Processing by Aerosol Multiphase Chemistry: Towards a Kinetic Modeling Framework of Secondary Organic Aerosol Formation in Aqueous Particles. *Atmos. Chem. Phys.* **2010**, *10* (17), 8219–8244. https://doi.org/10.5194/acp-10-8219-2010.
(18) Trainic, M.; Abo Riziq, A.; Lavi, A.; Flores, J. M.; Rudich, Y. The Optical, Physical and Chemical Properties of the Products of Glyoxal Uptake on Ammonium Sulfate Seed Aerosols. *Atmos. Chem. Phys.* **2011**, *11* (18), 9697–9707. https://doi.org/10.5194/acp-11-9697-2011.
(19) Yu, G.; Bayer, A. R.; Galloway, M. M.; Korshavn, K. J.; Fry, C. G.; Keutsch, F. N. Glyoxal in

Aqueous Ammonium Sulfate Solutions: Products, Kinetics and Hydration Effects. *Environmental Science & Technology* **2011**, *45* (15), 6336–6342. https://doi.org/10.1021/es200989n.
(20) Nozière, B.; Dziedzic, P.; Córdova, A. Products and Kinetics of the Liquid-Phase Reaction of Glyoxal Catalyzed by Ammonium Ions (NH_4^+). *The Journal of Physical Chemistry A* **2009**, *113* (1), 231–237. https://doi.org/10.1021/jp8078293.
(21) Rossignol, S.; Aregahegn, K. Z.; Tinel, L.; Fine, L.; Nozière, B.; George, C. Glyoxal Induced Atmospheric Photosensitized Chemistry Leading to Organic Aerosol Growth. *Environmental Science & Technology* **2014**, *48* (6), 3218–3227. https://doi.org/10.1021/es405581g.
(22) Herrmann, H.; Schaefer, T.; Tilgner, A.; Styler, S. A.; Weller, C.; Teich, M.; Otto, T. Tropospheric Aqueous-Phase Chemistry: Kinetics, Mechanisms, and Its Coupling to a Changing Gas Phase. *Chemical Reviews* **2015**, *115* (10), 4259–4334. https://doi.org/10.1021/cr500447k.
(23) Volkamer, R.; San Martini, F.; Molina, L. T.; Salcedo, D.; Jimenez, J. L.; Molina, M. J. A Missing Sink for Gas-Phase Glyoxal in Mexico City: Formation of Secondary Organic Aerosol. *Geophys. Res. Lett.* **2007**, *34* (19), L19807. https://doi.org/10.1029/2007GL030752.
(24) Kampf, C. J.; Jakob, R.; Hoffmann, T. Identification and Characterization of Aging Products in the Glyoxal/Ammonium Sulfate System – Implications for Light-Absorbing Material in Atmospheric Aerosols. *Atmos. Chem. Phys.* **2012**, *12* (14), 6323–6333. https://doi.org/10.5194/acp-12-6323-2012.
(25) McNeill, V. F.; Woo, J. L.; Kim, D. D.; Schwier, A. N.; Wannell, N. J.; Sumner, A. J.; Barakat, J. M. Aqueous-Phase Secondary Organic Aerosol and Organosulfate Formation in Atmospheric Aerosols: A Modeling Study. *Environmental Science & Technology* **2012**, *46* (15), 8075–8081. https://doi.org/10.1021/es3002986.
(26) Tsui, W. G.; Woo, J. L.; McNeill, V. F. Impact of Aerosol-Cloud Cycling on Aqueous Secondary Organic Aerosol Formation. *Atmosphere* **2019**, *10* (11), 666. https://doi.org/10.3390/atmos10110666.
(27) Woo, J. L.; Kim, D. D.; Schwier, A. N.; Li, R.; McNeill, V. F. Aqueous Aerosol SOA Formation: Impact on Aerosol Physical Properties. *Faraday Discuss.* **2013**, *165*, 357. https://doi.org/10.1039/c3fd00032j.
(28) Schwier, A. N.; Sareen, N.; Mitroo, D.; Shapiro, E. L.; McNeill, V. F. Glyoxal-Methylglyoxal Cross-Reactions in Secondary Organic Aerosol Formation. *Environ. Sci. Technol.* **2010**, *44* (16), 6174–6182. https://doi.org/10.1021/es101225q.
(29) Hritz, A. D.; Raymond, T. M.; Dutcher, D. D. A Method for the Direct Measurement of Surface Tension of Collected Atmospherically Relevant Aerosol Particles Using Atomic Force Microscopy. *Atmospheric Chemistry and Physics* **2016**, *16* (15), 9761–9769. https://doi.org/10.5194/acp-16-9761-2016.
(30) Bzdek, B. R.; Power, R. M.; Simpson, S. H.; Reid, J. P.; Royall, C. P. Precise, Contactless Measurements of the Surface Tension of Picolitre Aerosol Droplets. *Chem. Sci.* **2016**, *7* (1), 274–285. https://doi.org/10.1039/C5SC03184B.
(31) Gray Bé, A.; Upshur, M. A.; Liu, P.; Martin, S. T.; Geiger, F. M.; Thomson, R. J. Cloud Activation Potentials for Atmospheric α-Pinene and β-Caryophyllene Ozonolysis Products. *ACS Cent. Sci.* **2017**, *3* (7), 715–725. https://doi.org/10.1021/acscentsci.7b00112.
(32) Schwier, A. N.; Viglione, G. A.; Li, Z.; Faye McNeill, V. Modeling the Surface Tension of Complex, Reactive Organic–Inorganic Mixtures. *Atmos. Chem. Phys.* **2013**, *13* (21), 10721–10732. https://doi.org/10.5194/acp-13-10721-2013.
(33) Shapiro, E. L.; Szprengiel, J.; Sareen, N.; Jen, C. N.; Giordano, M. R.; McNeill, V. F. Light-Absorbing Secondary Organic Material Formed by Glyoxal in Aqueous Aerosol Mimics. *Atmos. Chem. Phys.* **2009**, *9* (7), 2289–2300. https://doi.org/10.5194/acp-9-2289-2009.
(34) Bateman, A. P.; Gong, Z.; Liu, P.; Sato, B.; Cirino, G.; Zhang, Y.; Artaxo, P.; Bertram, A. K.; Manzi, A. O.; Rizzo, L. V.; Souza, R. A. F.; Zaveri, R. A.; Martin, S. T. Sub-Micrometre Particulate Matter Is Primarily in Liquid Form over Amazon Rainforest. *Nature Geoscience* **2016**, *9* (1), 34–37. https://doi.org/10.1038/ngeo2599.
(35) Cappa, C. D.; Wilson, K. R. Evolution of Organic Aerosol Mass Spectra upon Heating: Implications for OA Phase and Partitioning Behavior. *Atmospheric Chemistry and Physics* **2011**, *11* (5), 1895–1911. https://doi.org/10.5194/acp-11-1895-2011.
(36) Virtanen, A.; Joutsensaari, J.; Koop, T.; Kannosto, J.; Yli-Pirilä, P.; Leskinen, J.; Mäkelä, J.

M.; Holopainen, J. K.; Pöschl, U.; Kulmala, M.; Worsnop, D. R.; Laaksonen, A. An Amorphous Solid State of Biogenic Secondary Organic Aerosol Particles. *Nature* **2010**, *467* (7317), 824–827. https://doi.org/10.1038/nature09455.
(37) Cheng, Y.; Su, H.; Koop, T.; Mikhailov, E.; Pöschl, U. Size Dependence of Phase Transitions in Aerosol Nanoparticles. *Nature Communications* **2015**, *6* (1). https://doi.org/10.1038/ncomms6923.
(38) Virtanen, A.; Kannosto, J.; Kuuluvainen, H.; Arffman, A.; Joutsensaari, J.; Saukko, E.; Hao, L.; Yli-Pirilä, P.; Tiitta, P.; Holopainen, J. K.; Keskinen, J.; Worsnop, D. R.; Smith, J. N.; Laaksonen, A. Bounce Behavior of Freshly Nucleated Biogenic Secondary Organic Aerosol Particles. *Atmospheric Chemistry and Physics* **2011**, *11* (16), 8759–8766. https://doi.org/10.5194/acp-11-8759-2011.
(39) Powelson, M. H.; Espelien, B. M.; Hawkins, L. N.; Galloway, M. M.; De Haan, D. O. Brown Carbon Formation by Aqueous-Phase Carbonyl Compound Reactions with Amines and Ammonium Sulfate. *Environ. Sci. Technol.* **2014**, *48* (2), 985–993. https://doi.org/10.1021/es4038325.
(40) De Vleeschouwer, K.; Van der Plancken, I.; Van Loey, A.; Hendrickx, M. E. The Effect of High Pressure−High Temperature Processing Conditions on Acrylamide Formation and Other Maillard Reaction Compounds. *Journal of Agricultural and Food Chemistry* **2010**, *58* (22), 11740–11748. https://doi.org/10.1021/jf102697b.
(41) Moreno, F. J.; Molina, E.; Olano, A.; López-Fandiño, R. High-Pressure Effects on Maillard Reaction between Glucose and Lysine. *J. Agric. Food Chem.* **2003**, *51* (2), 394–400. https://doi.org/10.1021/jf025731s.
(42) Schwarzenbolz, U.; Förster, A.; Henle, T. Influence of High Hydrostatic Pressure on the Reaction between Glyoxal and Lysine Residues. *Eur Food Res Technol* **2017**, *243* (8), 1355–1361. https://doi.org/10.1007/s00217-017-2846-x.
(43) Hamilton, J. F.; Baeza-Romero, M. T.; Finessi, E.; Rickard, A. R.; Healy, R. M.; Peppe, S.; Adams, T. J.; Daniels, M. J. S.; Ball, S. M.; Goodall, I. C. A.; Monks, P. S.; Borrás, E.; Muñoz, A. Online and Offline Mass Spectrometric Study of the Impact of Oxidation and Ageing on Glyoxal Chemistry and Uptake onto Ammonium Sulfate Aerosols. *Faraday Discussions* **2013**, *165*, 447. https://doi.org/10.1039/c3fd00051f.
(44) Hawkins, L. N.; Lemire, A. N.; Galloway, M. M.; Corrigan, A. L.; Turley, J. J.; Espelien, B. M.; De Haan, D. O. Maillard Chemistry in Clouds and Aqueous Aerosol As a Source of Atmospheric Humic-Like Substances. *Environ. Sci. Technol.* **2016**, *50* (14), 7443–7452. https://doi.org/10.1021/acs.est.6b00909.
(45) Jokinen, T.; Berndt, T.; Makkonen, R.; Kerminen, V.-M.; Junninen, H.; Paasonen, P.; Stratmann, F.; Herrmann, H.; Guenther, A. B.; Worsnop, D. R.; Kulmala, M.; Ehn, M.; Sipilä, M. Production of Extremely Low Volatile Organic Compounds from Biogenic Emissions: Measured Yields and Atmospheric Implications. *Proceedings of the National Academy of Sciences* **2015**, *112* (23), 7123–7128. https://doi.org/10.1073/pnas.1423977112.
(46) Kelly, J. M.; Doherty, R. M.; O'Connor, F. M.; Mann, G. W. The Impact of Biogenic, Anthropogenic, and Biomass Burning Volatile Organic Compound Emissions on Regional and Seasonal Variations in Secondary Organic Aerosol. *Atmospheric Chemistry and Physics* **2018**, *18* (10), 7393–7422. https://doi.org/10.5194/acp-18-7393-2018.
(47) Woo, J. L.; McNeill, V. F. SimpleGAMMA v1.0 – a Reduced Model of Secondary Organic Aerosol Formation in the Aqueous Aerosol Phase (AaSOA). *Geosci. Model Dev.* **2015**, *8* (6), 1821–1829. https://doi.org/10.5194/gmd-8-1821-2015.
(48) Apsokardu, M. J.; Johnston, M. V. Nanoparticle Growth by Particle-Phase Chemistry. *Atmospheric Chemistry and Physics* **2018**, *18* (3), 1895–1907. https://doi.org/10.5194/acp-18-1895-2018.
(49) Le Noble, W. J.; Miller, A. R.; Hamann, S. D. A Simple, Empirical Function Describing the Reaction Profile, and Some Applications. *J. Org. Chem.* **1977**, *42* (2), 338–342. https://doi.org/10.1021/jo00422a035.
(50) Asano, T.; Le Noble, W. J. Activation and Reaction Volumes in Solution. *Chem. Rev.* **1978**, *78* (4), 407–489. https://doi.org/10.1021/cr60314a004.
(51) Stokes, R. The Apparent Molar Volumes of Aqueous Ammonia, Ammonium Chloride, Aniline and Anilinium Chloride at 25°C and the Volume Changes on Ionization. *Aust. J. Chem.* **1975**, *28* (10), 2109. https://doi.org/10.1071/CH9752109.

598 **TOC**

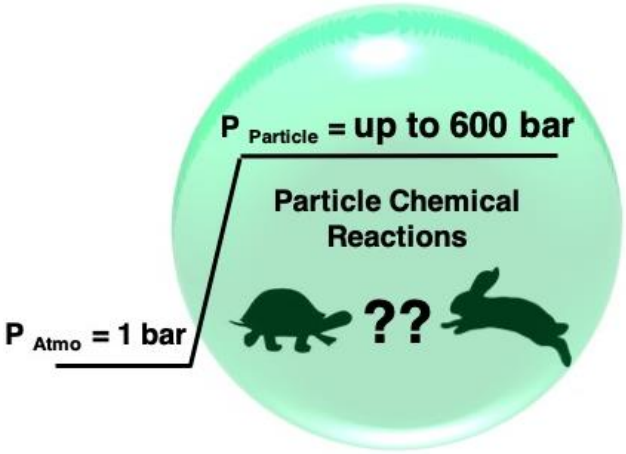
P Particle = up to 600 bar
Particle Chemical Reactions
??
P Atmo = 1 bar

599